

Bismuth telluride nanotubes and the effects on the thermoelectric properties of nanotube-containing nanocomposites

X. B. Zhao,^{a)} X. H. Ji, Y. H. Zhang, T. J. Zhu, J. P. Tu, and X. B. Zhang
 State Key Laboratory of Silicon Materials, Zhejiang University, Hangzhou 310027,
 People's Republic of China

(Received 23 July 2004; accepted 16 December 2004; published online 3 February 2005)

Nanotubes of quasilayered bismuth telluride compound were prepared by hydrothermal synthesis. Nanotubes have diameters smaller than 100 nm and spiral tube-walls. The low-dimensional morphology and hollow structure enable bismuth telluride nanotubes to be a potential thermoelectric material with a high figure of merit due to the efficient phonon blocking effect. The experimental results show that the addition of nanotubes leads to a remarkable decrease in the thermal conductivity with the electrical conductivity much less affected and thus to an increase in the figure of merit of the Bi₂Te₃-based material. © 2005 American Institute of Physics.
 [DOI: 10.1063/1.1863440]

Thermoelectric (TE) materials have many attractive applications in solid-state cooling and electric power generation. The property of a TE material is given by the figure of merit, $Z = \alpha^2 \sigma / \kappa$, or the dimensionless one, ZT , where α is the Seebeck coefficient, σ is the electric conductivity and κ is the thermal conductivity of the material, and T is the temperature. A good TE material should have a high σ like a crystalline material and a low κ like a glass, as suggested by Slack with the concept of "phonon-glass/electron-crystal" (PGEC) model.¹ Holey TE materials² such as skutterudites³ and clathrate crystals⁴ are typical TE materials having the crystalline nature of a PGEC. The basic crystal structures of these compounds ensure the good electric properties of the materials and the spacious voids or cages in the lattice structures reduce the thermal conductivity of the materials by the strong phonon scattering. Low-dimensional structures, such as nanowires and superlattice thin films,⁵⁻⁷ are another type of PGEC materials with glasslike low thermal conductivities due to the phonon-blocking effect of the nanostructures. Many advanced TE materials with high figure of merit have been reported in the last years, for example, partially filled skutterudites, Ba_{0.3}Ni_{0.05}Co_{0.95}Sb₁₂, with $ZT \geq 1.2$.⁸

Semiconducting bismuth telluride, Bi₂Te₃, and its alloys are the best TE materials available today near room temperature with the highest dimensionless figure of merit ZT of about 1.^{2,9} These materials, although have been used for more than 50 years, are of interest until now due to the potential to improve their ZT values by structural modification. For example, Kanatzidis *et al.* have prepared a cesium intercalated bismuth telluride (CsBi₄Te₆) with a high ZT at low temperature.¹⁰ The highest figure of merit even observed for TE materials was reported by Venkatasubramanian and co-workers with $ZT = 2.4$ at room temperature for p -type Bi₂Te₃/Sb₂Te₃ superlattice thin film.⁶ Preparation of nanostructured Bi₂Te₃ based alloys by low temperature routes, solvothermal or hydrothermal synthesis, has been also reported recently.¹¹ These chemical routes have the advantages of low synthesis temperature and fine grain sizes in comparison with those by a high temperature route such as melting process. Various morphologies of solvothermally or hydro-

thermally synthesized Bi₂Te₃ powders have been reported,¹² including nanorods, polygonal nanosheets, polyhedral nanoparticles, and sheet-rods. Novel fullerene-related structures like nanotubes would be very interesting to improve the TE properties of bismuth telluride based materials, since nanotubes possess both low-dimensional and holey structure features, and could be a hopeful PGEC material with high TE performance. Bi₂Te₃ has a quasilayered lattice structure. In each five atomic layers along the c -axis of Bi₂Te₃ there is a van der Waals bonding between two Te-layers. This makes it possible for Bi₂Te₃ to form a nanotube. Nanotubes, due to their hollow quasi-one-dimensional nanostructures and special physical, chemical and mechanic behaviors, have been intensively studied.¹³ However, most of those studies were focused on materials with layered lattice structures like graphite and synthesis processes like electric arc, laser ablation, and chemical vapor deposition. Here we report the hydrothermal synthesis of Bi₂Te₃ nanotubes and their promising effects on the improvement of the TE properties of Bi₂Te₃ based bulk material.

In a typical synthesis process, 30 mmol tellurium powder (5N purity, $\leq 30 \mu\text{m}$), 20 mmol BiCl₃ and 2 g ethylenediamine-tetra-acetic disodium salt (EDTA) were mixed with 400 ml distilled water in a teflon-lined autoclave with a capacity of 500 ml. Then 3.5 g NaOH and 3.5 g NaBH₄ were added in the solution. All chemicals used in the present work are analytical grade without further purification. The autoclave was sealed immediately and heated to the reaction temperature of 150 °C. During the reaction the solution was stirred by a stainless steel stirrer with a rotational speed of 100 rpm. After a reaction time of 24 h at 150 °C, the autoclave was cooled down naturally to room temperature. The precipitated dark grey powders were filtered, washed with distilled water, ethanol and acetone several times, and dried in vacuum at 100 °C for 6 h.

The phase structures were investigated by x-ray diffraction (XRD) with a Rigaku D/MAX-2550P diffractometer using Cu K_{α} radiation ($\lambda = 0.154056 \text{ nm}$). The powder morphology and fine structures were observed on a JEM-2010 transmission electron microscope (TEM) and a Philips-CM20 high-resolution TEM (HRTEM), respectively. The Seebeck coefficient α and electric conductivity σ were measured on a computer-assisted device. A temperature differ-

^{a)} Author to whom correspondence should be addressed. Electronic mail: zhaorb@zju.edu.cn; Fax: +86-571-87951171.

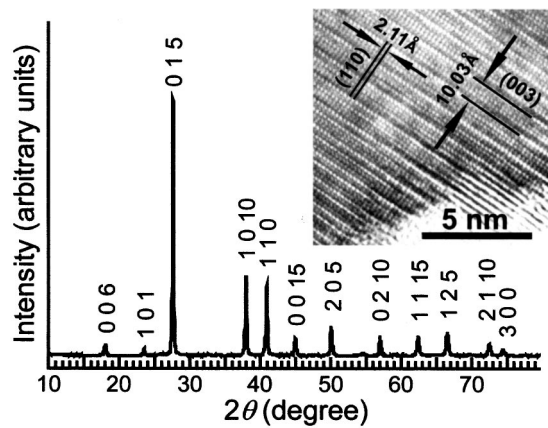


FIG. 1. XRD pattern and HRTEM image of the hydrothermally synthesized bismuth telluride.

ence of about 4 K between cool and hot ends of the sample was used for the Seebeck coefficient measurements. Four-point-probe method was adopted for the electric conductivity measurement. The thermal conductivity κ was calculated by using $\kappa = a\rho c_p$, where ρ is the sample density estimated by an ordinary dimension and weigh measurement at room temperature, a and c_p , the thermal diffusivity and specific heat of the sample, were measured on a Netzsch LFA-427 and DSC-404, respectively.

The XRD pattern in Fig. 1 indicates that the hydrothermally synthesized powders have a single rhombohedral lattice structure of Bi_2Te_3 (space group of $R\bar{3}m$). From the HRTEM image (inset in Fig. 1) the distances between two neighboring (110) faces and two (003) faces were estimated to be about 2.11 Å and 10.03 Å, respectively. The lattice parameters calculated from these measurements are $a = 4.22$ Å and $c = 30.09$ Å, which are slightly smaller than the standard data of JCPDS 82-0358, $a = 4.395$ Å and $c = 30.44$ Å.

The dominated morphology of the synthesized powder is nanotubes according to the TEM observations in Fig. 2. The sizes of tubes are about 30–100 nm in diameter and a few micrometers in lengths. The electron diffraction pattern taken from the three parallelly arranged tubes (Fig. 2, right upper) indicates that the tubes are single crystalline. From the HRTEM image of a Bi_2Te_3 nanotube, Fig. 3(a), we estimated the thickness of the tube wall being about 20 nm. Figure 3(a) shows also that the tube wall is not smooth and neat but uneven and spiral. The enlarged image of a small nanotube,

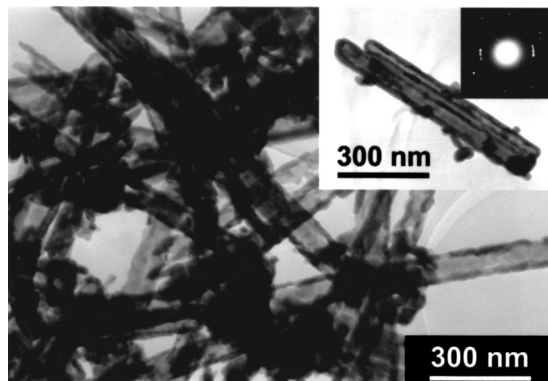


FIG. 2. TEM photos of the hydrothermally synthesized bismuth telluride nanotubes.

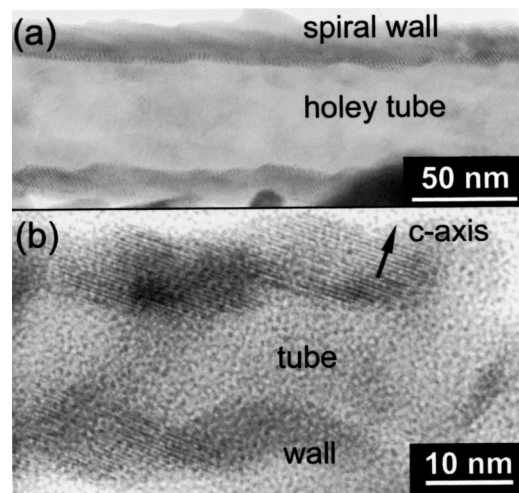


FIG. 3. HRTEM photos showing spiral walls of the bismuth telluride nanotubes with inclined (003) plane referring to the tube axis.

Fig. 3(b), reveals the typical crystalline structure of the tube walls. The c -axis of the Bi_2Te_3 rhombohedral lattice is at an angle of about 20° with the normal direction of the tube. The tilted atomic planes form a *spiral* wall like a continuously developed tape of pencil shavings as we can see also in Fig. 3(a). The formation of the spiral wall is considered to be originated from the *quasi*-layered structure of Bi_2Te_3 , since the synchronous growth of the five atomic layers is necessary for Bi_2Te_3 to form a tube with the base lattice plane being parallel to the tube axis like a carbon nanotube. A spiral wall consists of tilted atomic planes with ledges, which ensures the continuous growth of the tube.

Nanotubes have the structure features of both holey and low-dimensional materials: the hollow tube channels have a strong phonon scattering effect like the cages in a holey compound, one-dimensional nanotubes and two-dimensional tube-walls reduce the lattice thermal conductivity further due to the phonon blocking effect of their low-dimensional nature. These make Bi_2Te_3 nanotubes be an attractive TE material. As a primary application, we used the hydrothermally synthesized Bi_2Te_3 nano-structured powder as an additive of n -type Bi_2Te_3 TE materials. A zone-melted commercial n -type Bi_2Te_3 ingot was broken and milled to about 100 μm in size and then mixed with the hydrothermally synthesized nanotubes with the weight ratio of milled powder to nanopowder being 85:15. The mixed powder was hot pressed in vacuum at 350°C for 30 min using a pressure of 50 MPa in a graphite die with a diameter of 16 mm. The transport properties of the hot pressed bulk nano-composite (NC) samples were measured and plotted in Fig. 4 comparing with the data measured for the zone-melted (ZM) samples. The obvious difference of the Seebeck coefficient of the NC and ZM samples shown in Fig. 4(a) implies that the NC samples are stronger n -type conductive than the ZM sample, which is probably due to the additional heat treatment to prepare the NC samples and also the difference in chemical composition between the ZM sample and the nanotubes added in the NC samples. The stronger n -type conduction of the NC samples leads to not only a higher electrical conductivity of the NC samples than that of the ZM sample as shown in Fig. 4(b), but also the shift of the temperature of the apparent thermal excitation of minority carriers as well as the change of the semiconductor from n -type extrinsic to mixed conduction to-

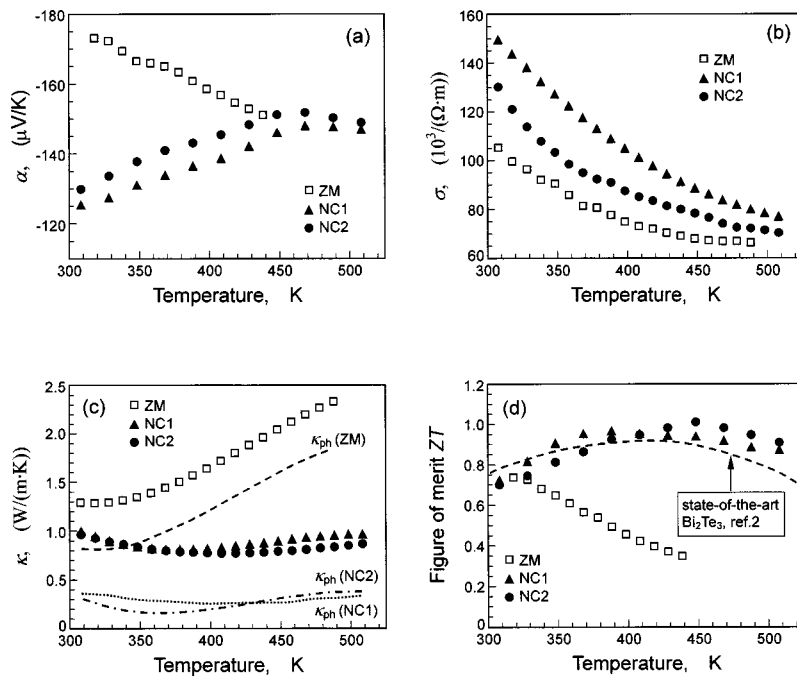


FIG. 4. Transport properties of the nano-composite samples (NC1, NC2) in comparison with the data measured from the zone-melted sample (ZM), for Seebeck coefficient (a), electrical conductivity (b), thermal conductivity (c), and the dimensionless figure of merit (d). The calculated phonon thermal conductivities, κ_{ph} , are drawn also in (c) for the ZM sample (dashed line) and both NC samples (dotted line and dashed-dotted line).

wards higher temperature as observed in Fig. 4(a) that the temperature of the maximum of the Seebeck coefficient moves from near room temperature for the ZM sample to about 470 K for the NC samples. It is of interest that the NC samples have much lower thermal conductivity and higher electrical conductivity than those for the ZM sample as shown in Fig. 4(b) and 4(c). The total thermal conductivity κ consists of the phonon contribution κ_{ph} and the carrier contribution κ_e which is related to the electrical conductivity σ with $\kappa_e = L_0 \sigma T$, where L_0 is the Lorenz number and approximately equal to $1.5 \times 10^{-8} \text{ V}^2 \text{ K}^{-2}$ in a nondegenerate semiconductor.⁶ Subtracting κ_e from the total κ , we find in Fig. 4(c) that the remaining phonon contributions, κ_{ph} , for the NC samples in Fig. 4(c) are about $0.3 \text{ W}(\text{m}\cdot\text{K})^{-1}$, which is about one fourth of that for the ZM sample. This means that the lattice thermal conductivity has been efficiently minimized by nanotubes. The result indicates that the nanostructuring leads to a remarkable decrease in the thermal conductivity with the electrical transport much less deteriorated. As shown in Fig. 4(d), the figure of merit of the NC samples is significantly higher than that of the ZM sample. The maximal figure of merit of the NC sample is above unity, which is not only significantly higher than that of the ZM sample but also well comparable to or even higher than that of the state-of-the-art Bi_2Te_3 alloys.² Also the temperature of the maximum of figure of merit moves from about 320 K for sample ZM to about 390 K for NC1 and 450 K for NC2, which is mainly related to the change of the temperature characteristics of the transport mechanism of the NC samples as discussed above. A higher figure of merit could be expected by the doping optimization of both nanotubes and the base alloy.

In summary, we present a new type of nanotubes of a quasilayered TE compound, Bi_2Te_3 nanotubes, prepared by hydrothermal synthesis. The low-dimensional morphology and holey structure enable Bi_2Te_3 nanotubes to be a potential TE material with a high figure of merit due to the efficient phonon blocking effect. The primary experiment shows that the nanotubes could improve the figure of merit of the Bi_2Te_3 based TE material efficiently.

The authors thank Dr. E. Müller, C. Stiewe, and W. Schönau, Institute of Materials Research, German Aerospace Center (DLR), D-51170 Köln, for the help on the measurements of some transport properties. This work was supported by the National Natural Science Foundation of China, Grant No. N50171064.

¹G. A. Slack and V. G. Tsoukala, *J. Appl. Phys.* **76**, 1665 (1994).

²T. M. Tritt, *Science* **283**, 804 (1999).

³B. C. Sales, D. Mandrus, and R. K. Williams, *Science* **272**, 1325 (1996).

⁴G. S. Nolas, D. G. Vanderveer, A. P. Wilkinson, and J. L. Cohn, *J. Appl. Phys.* **91**, 8970 (2002); D. X. Huo, T. Sasakawa, Y. Muro, and T. Takabatake, *Appl. Phys. Lett.* **82**, 2640 (2003).

⁵Y.-M. Lin, O. Rabin, S. B. Cronin, J. Y. Ying, and M. S. Dresselhaus, *Appl. Phys. Lett.* **81**, 2403 (2002); M. S. Sander, A. L. Prieto, R. Gronsky, T. Sands, and A. M. Stacy, *Adv. Mater. (Weinheim, Ger.)* **14**, 665 (2002); M. Martín-González, A. L. Prieto, R. Gronsky, T. Sands, and A. M. Stacy, *ibid.* **15**, 1003 (2003).

⁶R. Venkatasubramanian, E. Siivola, T. Colpitts, and B. O'Quinn, *Nature (London)* **413**, 597 (2001).

⁷T. C. Harman, P. J. Taylor, M. P. Walsh, and B. E. LaForge, *Science* **297**, 2229 (2002).

⁸X. F. Tang, L. M. Zhang, R. Z. Yuan, L. D. Chen, T. Goto, T. Hirai, J. S. Dyck, W. Chen, and C. Uher, *J. Mater. Res.* **16**, 3343 (2001); J. S. Dyck, W. D. Chen, C. Uher, L. Chen, X. F. Tang, and T. Hirai, *J. Appl. Phys.* **91**, 3698 (2002).

⁹F. J. DiSalvo, *Science* **285**, 703 (1999).

¹⁰D.-Y. Chung, T. Hogan, P. Brazis, M. Rocci-Lane, C. Kannewurf, M. Bastea, C. Uher, and M. G. Kanatzidis, *Science* **287**, 1024 (2000).

¹¹S. H. Yu, J. Yang, Y. S. Wu, Z. H. Han, J. Lu, Y. Xie, and Y. T. Qian, *J. Mater. Chem.* **19**, 8 (1998); Y. Deng, C. W. Nan, G. D. Wei, L. Guo, and Y. H. Lin, *Chem. Phys. Lett.* **374**, 410 (2003); X. B. Zhao, Y. H. Zhang, and X. H. Ji, *Inorg. Chem. Commun.* **7**, 386 (2004); X. B. Zhao, X. H. Ji, Y. H. Zhang, G. S. Cao, and J. P. Tu, *Appl. Phys. A: Mater. Sci. Process.* (in press).

¹²Y. Deng, X. S. Zhou, G. D. Wei, J. Liu, C. W. Nan, and S. J. Zhao, *J. Phys. Chem. Solids* **63**, 2119 (2002); Y. Deng, G. D. Wei, and C. W. Nan, *Chem. Phys. Lett.* **368**, 639 (2003); X. B. Zhao, X. H. Ji, Y. H. Zhang, and B. H. Lu, *J. Alloys Compd.* **368**, 349 (2004).

¹³S. Iijima, *Nature (London)* **354**, 56 (1991); C. Journet, W. K. Maser, P. Bernier, A. Loiseau, M. L. Chapelle, S. Lefrant, P. Deniard, R. Leek, and J. E. Fischer, *ibid.* **388**, 756 (1997); H. W. Zhu, C. L. Xu, D. H. Wu, B. Q. Wei, R. Vajtai, and P. M. Ajayan, *Science* **296**, 884 (2002); J. Goldberger, R. He, Y. Zhang, S. Lee, H. Yan, H.-J. Choi, and P. Yang, *Nature (London)* **422**, 599 (2003).